Green Chemistry

Supercritical CO_2-induced alteration of polymer-metal matrix and selective extraction of valuable metals from waste printed circuit boards

Journal:	*Green Chemistry*
Manuscript ID	GC-ART-07-2020-002521.R1
Article Type:	Paper
Date Submitted by the Author:	22-Aug-2020
Complete List of Authors:	Peng, Peng; Columbia University, Department of Earth and Environmental Engineering & Department of Chemical Engineering Park, Ah-Hyung; Columbia University, Department of Earth and Environmental Engineering & Department of Chemical Engineering

ARTICLE

Supercritical CO_2-induced alteration of polymer-metal matrix and selective extraction of valuable metals from waste printed circuit boards

vReceived 00th January 20xx,
Accepted 00th January 20xx

DOI: 10.1039/x0xx00000x

Peng Peng [a,b,c], Ah-Hyung A. Park [a,b,c] *

The rapidly accumulating amounts of waste electrical and electronic equipment (WEEE) is one of the biggest environmental concerns in modern societies, and this problem will be further accelerated in the future. The use of supercritical CO_2 ($scCO_2$) mixed with acids has been proposed as a greener solvent system compared to conventional cyanide and aqua regia solvents, however, the mechanisms of $scCO_2$ in metal extraction from WEEE are still poorly understood. Thus, this study focused on the physical, structural, and chemical interactions between $scCO_2$/acid solvents and complex layered components in waste printed circuit boards (WPCBs), one of the common WEEEs. Our study showed that the use of $scCO_2$-based pretreatment allows faster leaching of metals including copper (Cu) in the subsequent hydrometallurgical process using H_2SO_4 and H_2O_2, while allowing gold (Au) recovery as hydrometallurgically delaminated solids. This enhancement is due to the selective leaching of Ni and unique inner porous structures created by $ScCO_2$/acid treatment via dissolving the Ca-silicate-bearing fiberglass within the WPCB. Thus, the $scCO_2$-based pretreatment of WPCBs shows a multifaceted green chemistry potential relating to the reduction in solvent usage and targeted recovery of Au prior to shredding or grinding that would reduce any loss or dilution of Au in the subsequent waste stream.

1 Introduction

Due to the fast growth of the electronics industry, waste electrical and electronic equipment (WEEE), has become one of the most difficult challenges faced by humanity. Despite increasing efforts in recycling and reuse, a large fraction of WEEEs, such as waste printed circuit boards (WPCBs), are being disposed into the environment.[1,2] Furthermore, the amount of WEEEs being transferred/exchanged between states and countries (particularly to developing countries, as shown in Figure 1) are causing significant social and economic complications.[3-6] The exposed metals, plastics, and brominated organic flame retardants have led to various environmental and public health concerns around the globe.[7]

Spiked brominated organics (e.g. diphenyl ethers) have been observed the environment and in animal bodies, thus increasing the risk of food chain contamination and species endangerment.[8-11] Furthermore, elevated health risks have been associated with the growth and improper disposal of WEEEs, such as the high lead content in children's blood in developing countries.[12]

a. Department of Chemical Engineering, Columbia University, New York, NY 10027
b. Lenfest Center for Sustainable Energy, Columbia University, New York, NY 10027
c. Department of Earth and Environmental Engineering, Columbia University, New York, NY 10027
**Corresponding Author: ap2622@columbia.edu*
Electronic Supplementary Information (ESI) available: [details of any supplementary information available should be included here]. See DOI: 10.1039/x0xx00000x

Within the recycling chain of WEEEs, metal recovery from the WPCBs are considered as the most valuable stream for urban mining due to its higher metal content among WEEEs (Figure 2(a)).[13,14] Metals such as Cu, Ni, and Al are the main building blocks of the WPCBs, and precious metals including Ag, Au, and rare earth elements (REEs) are often used to build the connectors and various electronic components in the WPCBs (Table 1).[15-19] Therefore, there is a strong need to sustainably recycle the WPCBs and the increased significance of urban mining from WPCBs has become comparable to virgin mining.[20] The recovery of metals from WPCBs could provide a sustainable pathway to reduce the conventional mining and the landfilling of electronic wastes. The proper recycling of WPCBs could bring significant economic benefits since metals are valuable.[21,22]

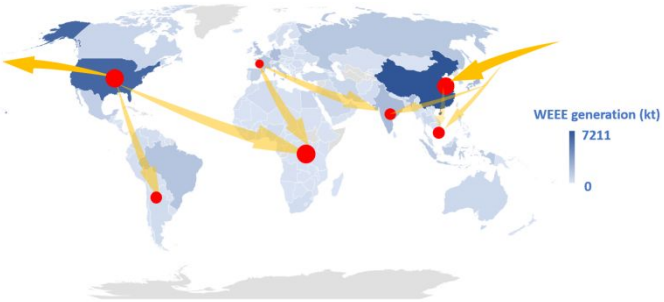

Figure 1 Global generation and transportation of Waste Electrical and Electronic Equipment (WEEEs), data and flow information extracted from references [3-6]

As shown in Figure 2 (b), the metal connectors contain a considerable amount of coated Au, which is the most important

ARTICLE

component within the WPCBs based on its value. In terms of total quantity, Cu is the most abundant metal that can be recovered. Common processes in the current WPCBs recycling industry start with energy-intense shredding and physical (i.e., density) separation to produce two crude streams, plastics and metals. The size reduction processes for WPCBs include shredding, grinding, and homogenization, followed by pneumatic or density separations.[23-25]

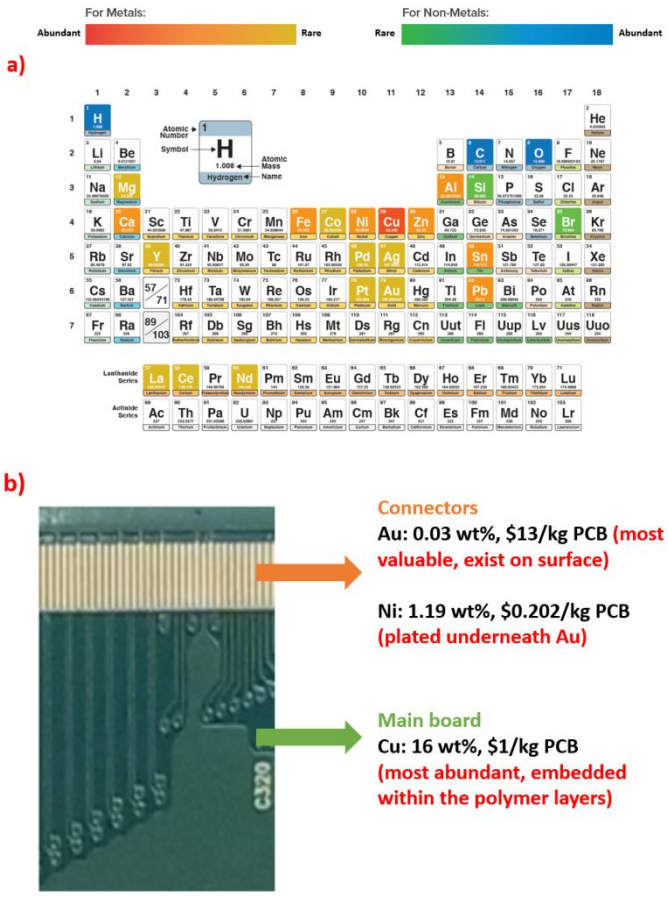

Figure 2 a) Periodic table of metal and non-metal resources in printed circuit boards (data extracted from references [3,15-18,26]); b) Average concentrations and values of major metals in printed circuit boards as well as their locations (data extracted from references[15-19])

Subsequently, the metal-rich streams are subjected to further refining via pyrometallurgical or hydrometallurgical pathways. Pyrometallurgy is considered to be environmentally hazardous due to the formation of toxic gas, slag and other insoluble industrial residues containing heavy metals.[27,28] Hydrometallurgy involves a series of acid or caustic leaching steps of WPCBs followed by metal recovery techniques such as electrowinning.[29] Thus, although hydrometallurgy is attractive in terms of its lower operating temperature and pressure compared to pyrometallurgical processes, it can also produce a large quantity of hazardous solvent wastes that need to be treated.[30] A majority of the past studies on WPCBs have been focused on the extraction of Cu, as it is the most abundant metal in WPCBs. [31-33]

Researchers have also attempted to develop ways to extract inert but precious metals (e.g., Au) from WPCBs, but often strong solvent systems have been used. Most well-studied solvents systems include cyanide, but has been gradually eliminated due to a number of drawbacks [3,34]. The disadvantages of cyanide include extremely high toxicity and corrosiveness. Further, cyanide has been reported to leach both Cu and Au, and thus, the overall cyanide consumption is very high if it is used for WPCBs. [29,35] Aqua regia is another alternative studied for extracting inert metals from WPCBs.[36,37] Unfortunately, it also shares similar disadvantages with cyanide such as environmental and public health concerns, high corrosiveness, volatility, toxic emissions, and low selectivity.[3]

In addition to the concentrated acids, the precious metal extraction from WPCBs using dilute hydrochloric acid has also been investigated.[38] Although the process was less hazardous compared with cyanide, aqua regia, or concentrated nitric acid, dilute acid solvents required long treatment times (> 22 hrs) to extract the metals.[38] Due to these limitations of acid leaching, studies have explored other hydrometallurgical routes to extract precious metals, utilizing chelating agents including thiosulfates [39-43] and thiourea.[44] Although thiosulfate is a relatively greener and less corrosive compared to concentrated nitric acid or aqua regia, the metal leaching using thiosulfate is challenged by its slow kinetics.[3]

In order to develop a greener alternative to recover the metals from WPCBs, we proposed to employ supercritical carbon dioxide ($scCO_2$) to enhance the extraction of metal contents from WPCBs.[3] As one of the most significant greenhouse gases, utilizing anthropogenic CO_2 in the WPCB treatment process could improve its overall sustainability. Besides this, the unique benefits of utilizing $scCO_2$ can be elaborated in three folds. First, $scCO_2$ can interact with various components of WPCBs such as metal layers, fiberglass, and polymers and leads to physical and chemical changes. Second, binary or trinary $scCO_2$-acid solvent systems (e.g., co-solvents such as water and ethanol) may be able to decompose, extract and separate halogen-containing polymeric compounds (e.g., Br and Cl in phenols and flame retardants[45]) and reduce the emission of toxic gases during the WPCB treatment.[46,47] Third, the $scCO_2$-acid treatment could extract metals from WPCBs with reduced acid requirement.

Our prior work with model system mimicking a WPCB, have shown that Cu could be effectively extracted from WPCBs using an acid (H_2SO_4) and $scCO_2$ mixture.[3] Another recent study has shown similar results with the addition of oxidant (H_2O_2) to the H_2SO_4/$scCO_2$ and ground WPCB system.[48] Unfortunately, both studies did not provide the fundamental understanding of chemical interactions between $scCO_2$ and different layered components of WPCBs and their resulted physical and chemical changes. The coupled mechanisms of transport and reaction phenomena of $scCO_2$-acid treatment as well as subsequent leaching processes should be investigated for the development of sustainable metal recovery technologies for WPCBs with highly heterogeneous layered structures of metal-polymer matrices.

Therefore, in this study, we aimed to develop a novel, staged process using $scCO_2$ with dilute acid and oxidant, and reveal the underlying mechanisms of how the novel staged $scCO_2$-acid solvent system could selectively extract base (i.e., Cu and Ni) and precious (i.e., Au) metals from WPCBs. In addition, the effect of $scCO_2$ on the mechanical and structural properties of different WPCB layers was investigated.

2 Experimental section

2.1 Methods and experimental set-up

There are a number of oxidative acids that can be used to leach metals from WPCBs, such as HCl and HNO_3 [33], and we selected H_2SO_4 and H_2O_2 since they have been reported to be the most cost effective for Cu leaching from WPCBs.[49] All the experiments were performed using H_2SO_4/H_2O_2 to be consistent and to isolate the effect of $scCO_2$. As shown in Figure 3, the $scCO_2$-acid treatment process investigated in this study consisted of two stages: (1st stage) the pre-treatment of WPCBs using the $scCO_2$-acid system and (2nd stage) metal leaching using the solvent containing acid (H_2SO_4) and oxidant (H_2O_2). Since the compositions of WPCBs are highly heterogeneous, the connector part of the WPCBs, which contains both Cu and precious metals (e.g., Au) was selected for this study. The LCD screen modules were collected from Columbia University's E-waste disposal center, and were manually dismantled to collect the WPCB connectors. The WPCB connector samples were cut to the size of 25 mm × 4 mm × 0.8 mm to meet the requirements of various characterization tools including the Dynamic Mechanical Analyzer. Figure 3 shows the solid and liquid samples collected at each stage.

Figure 3 A descriptive overview of the proposed two-stage $scCO_2$-induced waste printed circuit board (WPCB) treatment technology

During the first stage of the treatment, the WPCB sample was treated using $scCO_2$ and 1M H_2SO_4 in a Parr A5179 high pressure high temperature reactor, coupled with a Parr 4848 reactor controller for temperature control and monitoring (Figure 4). A Teledyne ISCO model 500 D syringe pump was used to supply $scCO_2$ to the reactor. 10 mL of 1M H_2SO_4 and WPCB samples were placed inside the batch reactor, and the system was first flushed with CO_2 in order to remove any oxygen. Next, the temperature and pressure of the system were adjusted to the desired values (150 bar, 120 °C), and maintained during the treatment while agitating the mixture at a rate of 250 rpm. Both liquid and solid samples were analyzed and the solid samples (both solid residue and delaminated solid shown in Figure 3) were collected for the second stage treatment study.

The second stage treatment, mainly targeting the metal extraction, employed 2 M H_2SO_4 at room temperature in the presence of the oxidizer, 0.2 M hydrogen peroxide (H_2O_2). After each stage of treatment, the samples were collected as shown in Figure 3.

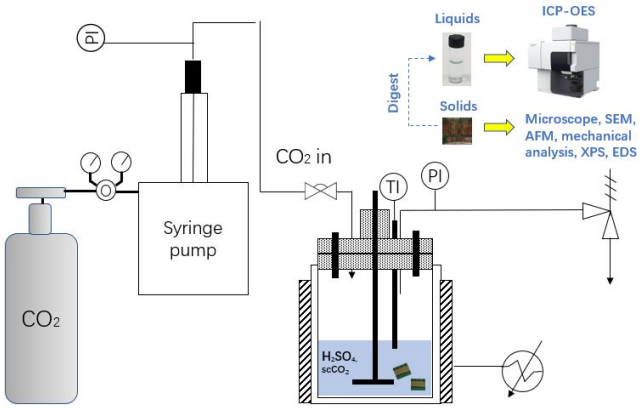

Figure 4 Flow diagram of the experimental setup for the 1st stage $scCO_2$ and acid pre-treatment of waste printed circuit boards

The liquid products from both stages were analyzed using Inductively coupled plasma-optical emission spectrometry (ICP-OES, Model 5110, Agilent, USA) to obtain the extents of metal extractions. The changes in the morphological, mechanical, and surface chemical properties of the delaminated solids and solid residue were determined using various characterization techniques described in Section 2.2. To accurately determine the total extraction efficiencies of various metals, solid residue and delaminated solid were ground and fully digested using aqua regia for 48 hours, and the resulting solutions were analyzed using ICP-OES.

2.2 Physical and chemical characterizations

Various characterization methods were employed to study the $scCO_2$-induced physical and chemical alterations of polymer-metal matrix within the WPCBs. First, close-up photos were taken using a Canon EOS Rebel SL2 Camera (Tokyo, Japan) to record the visual changes of the WPCB samples before and after the treatments. The brightfield microscope images (ZEISS AxioScope A1 (Oberkochen, Germany)) were also used to provide higher resolution views of physical alterations (Figure 5).

The Atomic force microscopy (AFM) (Model TT, AFM Workshop, USA) was employed to study the topological changes of the WPCB surface layers before and after the two-step treatments. After rinsing

ARTICLE

and cleaning, each sample was carbon taped on a steel sample holder, which was placed on the magnetic sample holder, with the top planner surface facing the tip. Next, the AFM tip was tuned to find the maximum amplitude of tip oscillation (resonance frequency ranging from 160 to 220 KHz). Then, the AFM was focused, and the tip position was adjusted to the proper distance from the sample surface so that it could detect Van Der Waals forces from the sample surface to start the scan. The AFM was performed on a 50 µm x 50 µm scan area, with the following test parameters, X Grain 100%, X Proportional 256, X integral 4096, Y Gain 100%, Y proportional 256, Y integral 4096, and Z setting 3. The AFM images were analyzed via the open-source Gwyddion Software to determine the height profile across the measured surface.

To examine microscopic changes on the surface of WPCB, a scanning electron microscope (SEM) (TT-2 manufactured by ZEISS SIGMA VP SEM) was used. Both planar and cross-sectional surfaces were studied in order to provide insights into the chemical and physical interactions between $scCO_2$-acid solvent and different WPCB layers. Cross-sectional SEM images were particularly interesting in showing how the $scCO_2$-incuded leaching during the first stage treatments affected the internal structure of the WPCBs. Note that when taking high-quality cross-sectional SEM images shown in Figure 6, the samples were coated with Au-Pd to avoid the charging effect caused by the lack of conductivity of the cross sections with high polymer content.

Flexural modulus was used to characterize and quantify the changes of the mechanical strength of the WPCBs. The mechanical property measurements were conducted using the DMA 850 Dynamic Mechanical Analyzer (TA Instruments, USA) based on the analysis method described by Licari et al.[6] The changes in the mechanical strengths were important due to its strong relation to the energy consumption during the physical shredding and grinding that are often required for e-waste pre-treatment. For the surface chemical changes, X-ray photoelectron spectroscopy (XPS) was used to identify both metals and non-metals on solid products obtained from each treatment stage. The Handbook of XPS by the Physical Electronic Division from the Perkin-Elmer Corporation[50] was used to specify the elements, unless noted. The cross-sectional elemental compositions were determined by a Bruker XFlash® 6|30 Energy-dispersive X-ray spectroscopy (EDS) detector (MA, USA) coupled with the SEM analysis. These surface characterization results were combined with the ICP-OES data to provide insights into the metal extraction mechanisms during the proposed two-step $scCO_2$-acid WPCB treatment process.

3 Results & Discussions

3.1 Physical changes of planar surface of WPCB connector during $scCO_2$-acid pre-treatment and the 2nd stage leaching

Most of the recently-manufactured WPCB connectors have a surface protective organic layer to enhance the durability and longevity of the connector.[51] A semi-transparent layer was also visibly detected on our WPCB connector samples as shown in the brightfield microscope image (Figure 5(a1)). According to the XPS analysis shown in Section 3.4 (Figure 10(a1)) and data found in literature,[52-54] the protective layer is a silicon-based, long-chain phenolic epoxy resin that is used to provide blister resistance and flame retardancy for the WPCBs. This surface protective organic layer experienced swelling after the first stage treatment using $scCO_2$ and H_2SO_4 as evidenced in microscope image (Figure 5(b1)), AFM image (Figure 5(b2) and SEM images (Figures 5(b3) and 5(b4)). After the second stage treatment using H_2SO_4 and H_2O_2,

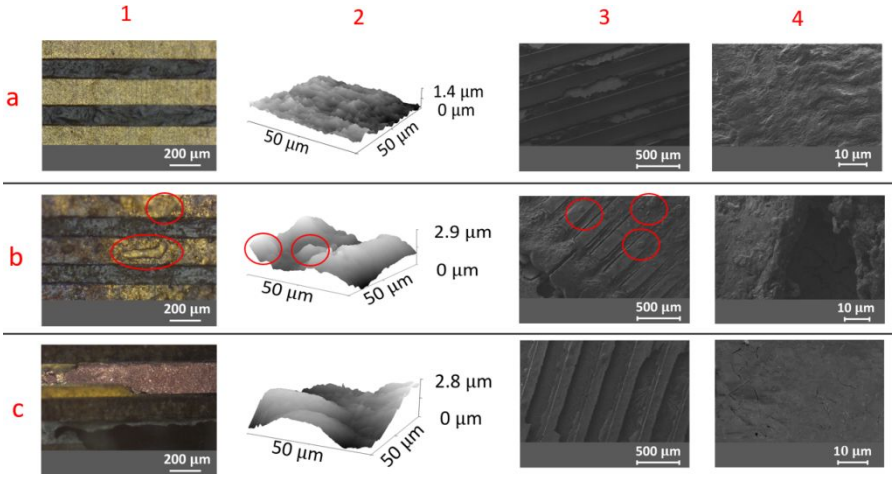

Figure 5 Brightfield microscope images (1), AFM topographies (2), and SEM images (3 and 4) of the upper surface of a) untreated waste printed circuit board (WPCB); b) WPCB after 1st stage $scCO_2$/acid treatment; c) WPCB after 2nd stage acid/oxidant treatment

Figure 5(c1) shows further damage on the protective layer. These images indicate a strong correlation between the existence of the protective layer and the delamination performance of metals, as the unextracted Au mostly remained under the residue protective layer (Figure 5(a1) versus Figure 5(c1)).

While the brightfield microscope images show detailed surface changes via color and transparency differences, SEM images provide higher resolution characterizations of WPCB connector samples. For example, the SEM image in Figure 5(a3) shows that the patches of light colored areas where the surface coating is missing (manufacture flaws or damages caused by the initial processing of this study). These uncoated/unprotected spots may have provided the necessary channels for $scCO_2$ or the H_2SO_4 to penetrate and interact with Au and the plastic-metal matrix underneath.

During the first stage treatment, the organic protective surface layer swelled and foams were formed, as indicated in Figure 5(b1)-5(b3). The thickness of the protective layer almost doubled and surface cracks (10 to 40 μm in scale) were observed as shown in Figure 5(b4). According to our previous study, the foaming, swelling, and fracturing of the surface protective silicon-based epoxy resin layer were mainly caused by $scCO_2$ via physical alterations via free volume expansion and it was not a chemical change.[3] These behavior are similar to those found in simpler polymer-CO_2 systems.[55,56] The structure underneath the fracture (Figure 5(b4)) was similar to that observed at the fractured Au electro-deposited surface reported in previous literature.[57]

After the second stage acid/oxidizer treatment, the protective layer became further fractured, and more importantly delaminated (Figure 5(c1)). The fracture propagation and delamination in the second stage was caused by the osmotic cracking, as well as the interphase and interfacial debonding as the solvent penetrated into the plastic matrix through the fractures.[58,59] SEM images in Figures 5(c3) and (c4) also shows the development of fractured structures. The analyses of the liquid samples also revealed that the Ni layer between the Cu and Au-rich layers was extracted during the first stage treatment, and this could be another cause of the partial delamination of Au and Cu etching observed in Figures 5(b1)-5(b4). More discussions on the metal leaching and its associated effect on the morphological changes are given in the subsequent sections.

The AFM images revealed the 3D surface topography changes of the WPCB connectors during each stage of the treatment. Figure 5(a2) shows that the topography of the untreated WPCB connector was relatively smooth, with a small height variation of less than 650 nm. After the first stage treatment, the distinct swelling features are better observed in the topography image shown in Figure 5(b2). The AFM topography offered a more quantitative description of the foaming and swelling of the surface protective layer, which agreed with the surface SEM results shown previously. The largest height variation across convex surface increased to over 2 μm, with smaller bubble-like structures ranging from 200 nm to 1 μm in heights, which were shown as the swollen irregular surfaces highlighted with red circles in Figures 5(b1) and (b2). After the second stage treatment, acid-etched deeper surface structures were found (Figure 5(c2)). The reported thickness of the organic protective layer is in the range of 0.2 to 0.4 um [60,61] which are similar to those found in our study.

3.2 Chemical interactions of $scCO_2$-acid system with different WPCB layers creating structural and mechanical changes and altered leaching behaviors

The physical and chemical changes of the planar surface of the WPCB connector was particularly important in terms of Au recovery but most of Cu (the second valuable metal in WPCBs) are embedded in the inner layers of WPCB connectors. Thus, the exposed inner cross-sectional surface of the WPCB connector was investigated throughout the proposed two stage treatment. Both close-up photos and SEM images in Figure 6 clear show layered structures of WPCB connectors and how they became altered during each treatment step.

The most noticeable differences in the cross-sectional views of the WPCB connectors were swelling, disordering of structures and the development of large pores. The thickness of the WPCB connectors increased by nearly 30 vol.% (examples shown in Figure 6(a1) of 0.66 mm (untreated) to Figure 6(c1) of 0.84 mm (after the second stage treatment)). The internal structure of the untreated WPCB connectors consists mainly of two forms of structures, solid and rods, with relatively smooth textures (Figures 6(a2) and 6(a3)). After the first treatment using $scCO_2$ and H_2SO_4, the formation of micron-scale pores in the cross-sectional region was observed (Figure 6(a3) versus 6(b3)). The formation of these pores was critical for our proposed enhancement of acid penetration into the metal-polymer matrix in the presence of $scCO_2$, and the metal recovery data in the section 3.3 supports our proposed WPCB treatment scheme.

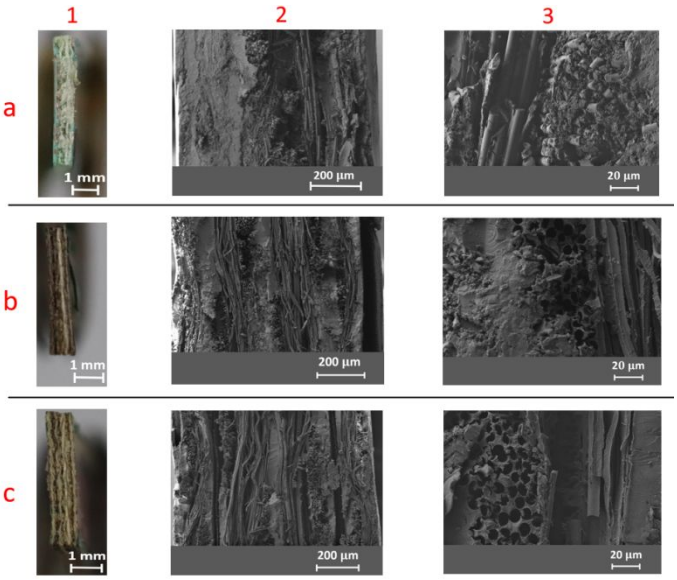

Figure 6 Closed up photos (1), cross-sectional SEMs (2 and 3), of the a) untreated WPCBs; b) WPCBs after 1st stage treatment; c) WPCBs after 2nd stage treatment

But the main fundamental question was how these pores were created. The development of these pores was first hypothesized by the free volume expansion of the polymeric layer caused by the sorption of $scCO_2$. However, the pores found in literature reporting

ARTICLE

$scCO_2$-polystyrene systems were in the range of nanometers,[62] which is orders of magnitude smaller than the ones found in our study. Thus, overall the sorption of $scCO_2$ would impact the permeability of $scCO_2$-acid solvents into the WPCB matrix but would not be the main mechanism of the large pore generation.

The distinct features of large pores (in the scale of 7 to 10 μm) can be found in the WPCB sample collected after the second stage acid/oxidant leaching step (Figure 6(c3)). Comparing the SEM images, it was concluded that the pores were likely created due to the extraction of the outpointing fiberglass rods during each treatment step. According to the literature, the diameter of the fiberglass used in the manufacturing of WPCBs is in the range of 7 – 10 μm, which matched the pore diameter. Chemical analyses presented in section 3.3 provide additional evidence for these findings.

Besides the enhanced extraction and separation of the metals, another proposed advantage of the $scCO_2$-based WPCB treatment scheme was the reduction in grinding energy. WEEEs including WPCBs are complex in terms of materials, and their polymeric and metallic parts make them less brittle and more ductile. Therefore, the size reduction process that is needed for the physical separation and the hydrometallurgical metal extraction is energy intensive and different from conventional grinding processes of mineral ores.[3,28,63] The formation of porous structures within the internal volume of the WPCBs and potential chemical alteration of polymers in the presence of $scCO_2$ and heat were proposed to change in their mechanical strength. The negative correlation between the porosity and the mechanical strength of plastics such as epoxy was demonstrated in previous literature,[64,65] which was also observed in this study (Figure 7).

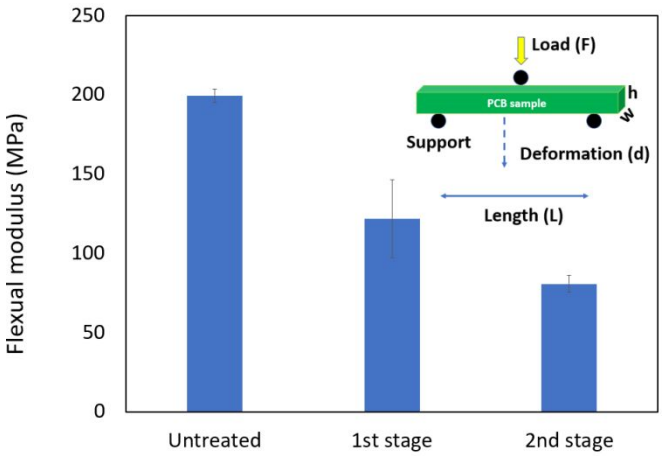

Figure 7 Changes in the flexural modulus of WPCBs before and after the two-stage $scCO_2$-induced treatment

One of the ways to characterize the mechanical strength of ductile materials under high shear treatment, such as shredding, is the use of flexural modulus.[6] Equation (1) can be used to estimate the flexural modulus as a function of the given load and the measured deformation of the material.[6]

$$\text{Flexual modulus} = \frac{L^3F}{4wh^3d} \quad (1)$$

As shown in Figure 7, the measured flexural modulus was reduced by up to 60% after the two-stage $scCO_2$-based WPCB treatment. This is a very promising result in terms of the overall energy requirement for WPCB treatment, and thus, the size reduction of WPCBs should be designed and added to the right step considering the changes in the mechanical strength.

3.3 Metal recovery from $scCO_2$/acid treated WPCBs

As illustrated in Figure 3, metals in WPCBs are recovered in two phases, delaminated solids and dissolved species in the liquid phase. The target metals in this study were Au, Ni, and Cu. As mentioned, these metals are disproportionately distributed throughout WPCBs, but in average, they accounted for 0.01 wt%, 1.1 wt%, and 23 wt% of our WPCB samples, respectively. As expected, Au was recovered as solids in the delaminated solid product, while Cu was recovered via leaching into the solvent phase. Figure 8 summarizes the recovery rates of the major metals (i.e., Au, Cu, and Ni) and the rates from this study are compared to those in the literature with solvents with different green factors. Interestingly, the extraction rates of Cu and Ni were favored in different stages within our process. Cu was selectively extracted during the second stage of treatment while Ni was mostly extracted in the first stage of the $scCO_2$/acid pre-treatment. They were different by orders of magnitude suggesting that effective separation between Cu and Ni may be possible through this two-stage WPCB treatment process.

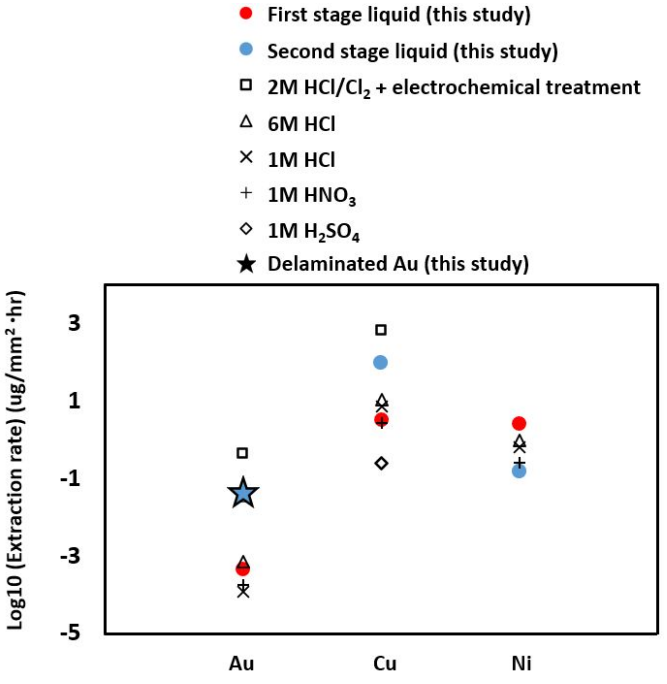

Figure 8 Metal recovery rates normalized to the top plane surface area for Au, Ni, and Cu recovery rate determined using the reactive cross-sectional area. These surface areas were selected based on their distribution within the WPCB. Estimated literature data are given as comparison.[38,68]

During the first stage $scCO_2$/acid pre-treatment (red circle data points in Figure 8, the high extent of Ni recovery in the pre-treatment of relatively large WPCB pieces used in this study was because Ni mostly exists on the surface of the WPCB along with Au and some literature have reported that Ni leaching can be enhanced at high temperature and pressure in the presence of acid (e.g., H_2SO_4).[66] The extraction of Ni seems to influence the leaching behavior of other metals in the subsequent stage. Unlike the metal recovery from natural ores, the e-waste processing technologies are challenged by the interferences between different metal leaching and separation processes.[3,63] The selective extraction of Ni and Au, during the first stage treatment and delaminated solid, illustrates the benefits and potential opportunities for the $scCO_2$-acid pre-treatment process.

In the second stage (blue circle data points in Figure 8, the pre-treated WPCB was processed using a typical hydrometallurgical process using the acid-oxidizer mixture.[67] As expected, Cu extraction was significantly enhanced in H_2SO_4+H_2O_2 solvent and additional debonding of Au coating was observed. The black star in Figure 8 marks the delamination rate of Au from the surface of WPCB (i.e., solid separation product).

As shown in Figure 8, the extraction rates for Cu and Ni, were higher than most reported values in literature that investigated the extraction of metals from ungrounded WPCB pieces. This was the case even compared to the study with the most concentrated acid solvent (6M HCl).[38] Particularly, the Ni extraction from the WPCB surface was very effective. Over 87.5% of Ni was extracted during the first stage $scCO_2$/acid treatment, and after the second stage, nearly 97.4% of Ni was extracted from WPCB. On the other hand, the extraction of Au was favored in the second stage. Its leaching was minimal in the first stage, but the overall extent of Au recovery after the second stage was nearly 96.6%. These results show that Ni and Au can be selectively extracted from WPCB. Since Au was recovered as delaminated solids, the separation of Au and base metals was straightforward.

The time required for full recovery of metals in this study was significantly shorter than literature values obtained using oxidative acids (i.e., HCl and HNO_3 for 10 hours[38]) and weak organic acids (i.e., acetic acid and citric acid for 100 hours[38]). As shown in Figure 8, only prior study performed better than this study in terms of metal recovery was the electrochemical treatment of WPCB using HCl/Cl_2 (black open square).[68] The main difference between this electrochemical treatment and our $scCO_2$-based solvent treatment was that the electrochemical treatment continuously produced strong oxidant (Cl_2) in-situ during the metal extraction and this allowed rapid extraction of Au and Cu. The recovered Au was in the form of dissolved species in the liquid phase, whereas our process recovers Au as solids. It is also important to consider the sustainability of each treatment process. Although chlorine leaching tends to have faster leaching kinetics, the use of strong oxidant such as Cl_2 requires extensive corrosion protection and emission controls for safety.[69,70]

As discussed earlier, the selective extraction of Au as delaminated solid is one of the benefits and potential opportunities for the $scCO_2$-acid pre-treatment technology. Other studies have reported that 50% to 90% of precious metals including Au were lost through the plastic and particulate waste streams during the size reduction and physical separation of WPCBs (e.g., shredding, grinding, and density separation).[71-73] Since Au mainly exists on the surface layer of WPCB,[15-19] recovering it before shredding and grinding would be more effective instead of diluting it into other waste streams.

Since unlike Au, Cu is widely distributed throughout the volume of the WPCB polymer matrix, the treated WPCB was ground once Au was recovered. Leaching experiments were performed using ground WPCB particles to obtain the reaction kinetics and the total extent of Cu extraction behaviors from WPCBs. As shown in Figure 9, the rate of Cu leaching from WPCB particles increased 5 times when WPCB was pre-treated with the $scCO_2$/acid system, which was also significantly higher than the rates achieved by the recently-published studies using novel solvent systems (i.e., $Fe_2(SO_4)_3$ solvent[74] and NH_4OH+H_2O_2 solvent[75]). With the $scCO_2$/acid pre-treatment, we were able to extract more than 90% of Cu from WPCB particles within 20 min, which is a very promising result compared to the previously reported data. The total Cu recovery from WPCB particles was 99.998% after the two-hour leaching process. Both the partial replacement of strong acid with $scCO_2$ and reduced solvent requirement based on faster reaction kinetics would contribute positively towards the green chemistry principles.

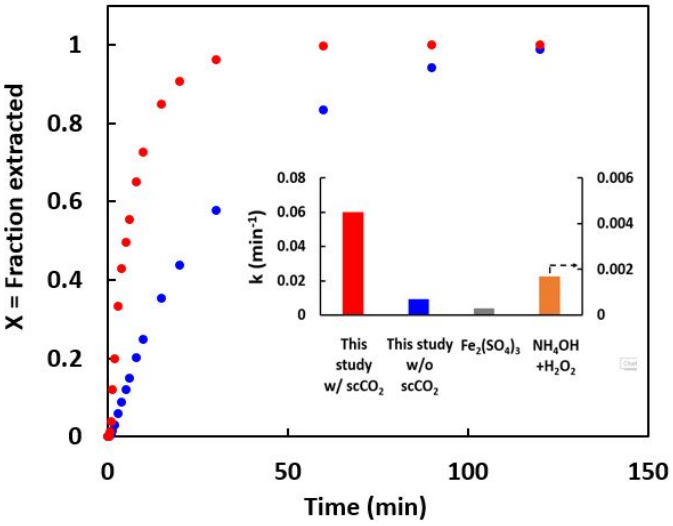

Figure 9 Effect of the $scCO_2$/acid pre-treatment on leaching kinetics of Cu from ground waste printed circuit boards. Solvent contained H_2SO_4+H_2O_2 and the leaching was performed under room

temperature. Inset Figure shows the rate constant (k) of Cu initial leaching from WPCB. The data from this study obtained with (red data set) and without (blue data set) $scCO_2$/acid pre-treatment were compared to two most recent data in literature (i.e., $Fe_2(SO_4)_3$ solvent[74] (grey bar) and $NH_4OH+H_2O_2$ solvent[75] (orange bar))

3.4 Hydrometallurgical delamination of Au and Leaching behaviors of base metals from upper WPCB surface

As discussed earlier, one of the unique features of the two-step WPCB treatment involving $scCO_2$ was the recovery of Au a solids. In case of leaching experiments performed using larger WPCB pieces, most of the leaching occured on the surface of the WPCB sample, and thus, the surface chemical characterization was carried out using the XPS in order to probe the mechanisms of metal leaching. As expected, the Au 4f peaks between 85 to 90 eV was observed (Figure 10 (a1)). However, the intensity of the peaks were very low. Also note that here, a slight peak shift was observed for the C1s peak from 284 eV, which corresponds to the relatively larger presence of ether, ketone, carboxyl, and carbonates, which are often used in epoxy resins or plastics in the PCBs. Meanwhile, the carbon peaks, from the C1s peak at 288 eV and the C KVV peaks at around 990 eV had strong intensities, indicating the high carbon content in the surface protective layer. As shown in Figure 10 (a2), for the untreated PCB connectors, the Au coating that covered the connectors for conductivity and durability purposes was detected. The thickness of the silicone-based organic protective layer on the Au layer was relatively large to the XPS penetration depth. Therefore, the Au peaks were not detected at the protected surface.

After the first stage of treatment (Figure 10(b1)), the splitted Au 4f peaks between 85 to 90 eV was replaced by a single peak at 79 eV, which represented Cu 3p, and its possible overlapping with Al 2p.[67] Besides Au, Cu was observed on the surface of the PCB after the first stage $scCO_2$/acid treatment. The exposure of Cu on the surface after the first stage treatment was caused by the fracture of the Au coating layer.[16] We also characterized the surface of the delaminated solid samples obtained from the first stage treatment. Their XPS spectrum (shown in Figure 10(b2)) indicated the presence of high concentrations of Si and C (i.e., various organic components). These fine solid materials were mostly from the exposed cross-sectional area, where plastic and fiberglass components exist (shown in Figure 4(a1) and 6(b1)), during the $scCO_2$/acid treatment. Limited studies have shown the interactions between $scCO_2$ and polymers as well as fiberglass and potential mechanical degradation of PCBs. [45, 68, 69]

All the solid products (both large solid residue and delaminated solids) from the first stage $scCO_2/H_2SO_4$ treatment was used to carry out the second stage treatment involving $H_2SO_4+H_2O_2$ solvent. As shown in Figure 6, significant amounts of metals (Ni and Cu) were extracted in this stage, and thus, the surface concentrations of these metals after the second stage treatment were lower. The carbon and oxygen peaks were intensified, indicating the major presence of organic components in final solid residues. The spectrum for the solid residue, Figure 10(c1) showed that the treatment of sulfuric acid and hydrogen peroxide revealed more metals underneath the delaminated Au, such as Mg and Cu, due to the interfacial fatigue crack initiations and adhesional failure in the gold and polymer composites mentioned previously. Since Au is not soluble, it remained in the delaminated solid, and was confirmed by the Au 4f peaks. Its relative intensity was higher than that for the untreated PCB surface, concluding that our two-stage treatment was able to concentrate Au in the delaminated residue stream, which agreed with the ICP-OES results, as discussed in Figure 6(a).

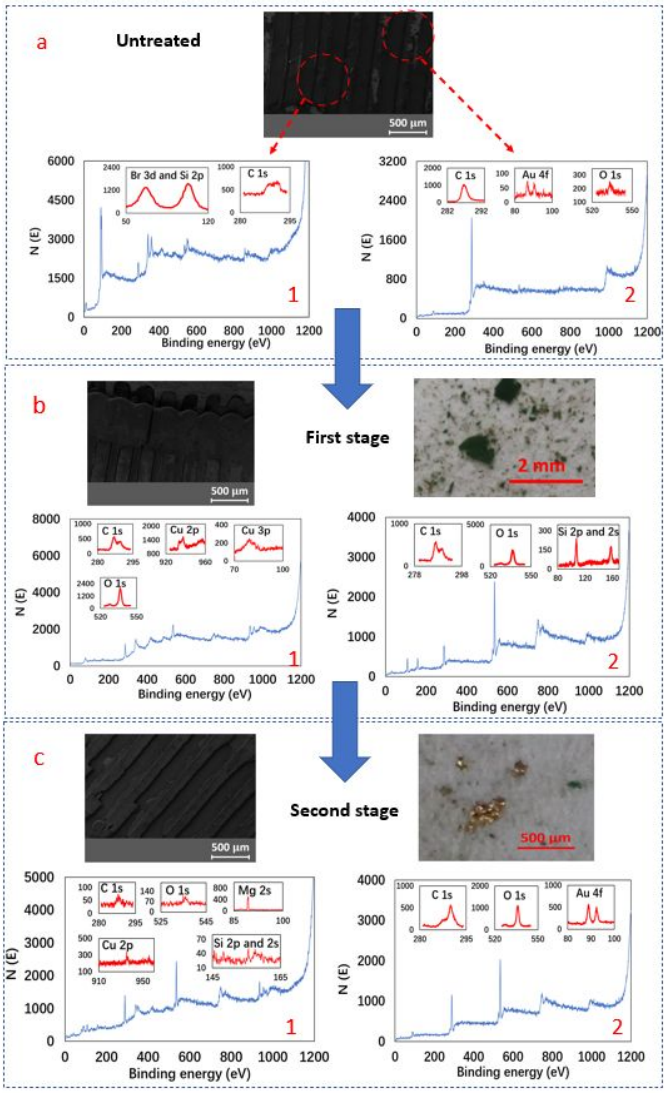

Figure 10 XPS diagrams of the a) untreated WPCB; b) solid residue after 1st stage treatment; c) metallic part of delaminated extracts after 2nd stage treatment, and d) the solid residue after 2nd stage treatment

3.5 Leaching behaviors of different components in cross-sectional WPCB layers

As discussed in Section 3.2, WPCB has very complex layered structures, and thus, their leaching behavior are very different depending on what exposed layer contains. Thus, in addition to the Au-rich surface area analysed in Section 3.4, the changes in the cross-

sectional area of WPCB samples during the two-stage treatment was studied using EDS mapping matched with the SEM images.

As shown in Figure 11 (a), parallel distribution patterns between the plastic (i.e., Carbon) and Cu layers were visibly identified. Within the general design of both traditional and modern WPCBs, the internal Cu layer serves as the ground and connections for the various electronic parts on the surface and internal structure of the WPCBs.[82,83] Interestingly, the existence of anti-flame Br-bearing compound was uniform across the board rather than a surface layer. The removal and capture of Br is very important during WPCB treatment and recycling in terms of environmental and health concerns. The wide distribution of Br identified in this study illustrates the potential challenge of WPCB management technologies. The EDS results of the cross-sectional WPCB layers also confirmed the existence of the internal vertical and horizontal fiber rods mainly consisting of Si, Ca, and Al. Thus, the dense-packed rods should be fiberglass and epoxy resins that include CaO and aluminosilicate to insulate the internal Cu layers while holding different WPCB layers together.[84]

The major unique difference observed in Figures 10(a) and 10(b) is the disappearance of Ca, Al and Si during the first stage $scCO_2/H_2SO_4$ treatment. The $scCO_2$+acid reacted with fiberglass exposed in cross-section surfaces and leached out Ca, Al and Si. According to the ICP analysis of the liquid product, a small fraction of Ca and Al in the liquid phase re-precipitated out as $CaSO_4$ and $Al_2(SO_4)_3$. The formation of these precipitates were also reported in literature.[85] The XPS results given in Figure 10(b2) shows the derivative peaks of Si 2P (100 eV), indicating the existence of Si from fiberglass as SiO_2. Also, the relatively strong Si 2S peak at 156 eV indicates the presence of siloxane (Si-O-Si).[50] The siloxane complex Si–O–Si network was also reported in literature during corrosion reactions of fiberglass with acids, forming products including H_4SiO_4 and SiO_2, which were partially soluble in acids and would precipitate under low pH conditions.[86-88]

These findings confirm our earlier discussion on the development of large micron-size pores due to the dissolution of fiberglass. Since the arrangements of the fiberglass and metal layers are directional, the leached surface continued to show elements including Ca, Si and Cu, which were in the exposed inner layer. The main disappearance of the Ca and Si in the elemental mapping was associated with the horizontal, outpointing fiberglass rods. The second stage treatment using H_2CO_4/H_2O_2 continued to remove inner Ca, Si and Cu. In the case of Br, its wide distribution did not change and it seems that Br remained in its original polymeric form and not leached into the solution phase. Thus, the capture and separation of Br can be focused on the solid residue that was high in polymeric components of WPCBs.

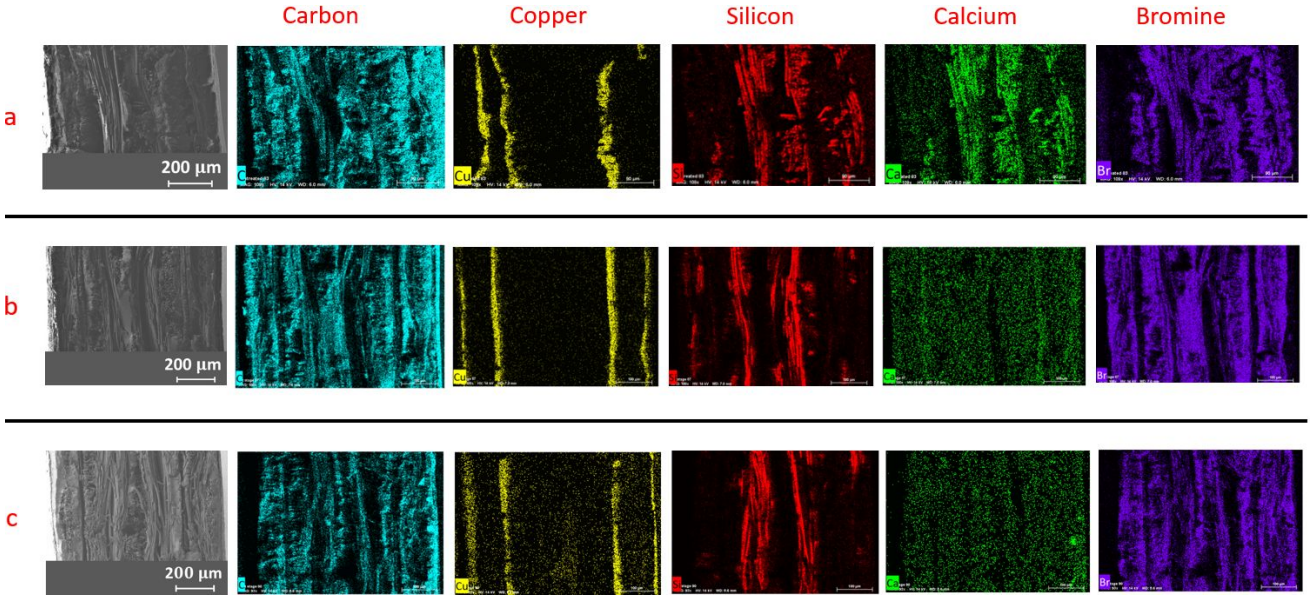

Figure 11 EDS cross-sectional mapping results of the a) untreated WPCB, b) WPCB after the 1st stage treatment; c) WPCB after the 2nd stage treatment

3.6 Proposed scheme of metal recovery from WPCBs via supercritical CO_2 treatment

Based on the delamination and leaching behavior of metals found in this study, the alteration and separation mechanisms of the WPCBs via the proposed two-stage $scCO_2$-based WPCB treatment process are illustrated in Figure 12. First, Ca and Al in the fiberglass were extracted into the liquid phase via the dissolution reaction at the low pH condition in the $scCO_2/H_2SO_4$ solvent and the dissolved Ca and Al remained in the solvent system or re-precipitated out as $CaSO_4$ and $Al_2(SO_4)_3$. The dissolution of Ca and Al-bearing rods created large (micron-sized) directional inner pores, which allowed $scCO_2$ and H_2SO_4 to penetrate the WPCB structure. Factures were also observed as vertically aligned Ca and Al-bearing rods were dissolved in the solvent environment and fine particles rich in Si

(H_4SiO_4 and SiO_2) were collected during the first stage treatment, along with some deformed plastics.

Due to the treatment of $scCO_2$, the organic surface protective layer became swollen and fractured, forming a foam-like structure on the surface of the WPCB. This allowed the penetration of $scCO_2$/acid solutions into the WPCB to interact with the metal beneath the organic coating. In this stage, a majority of surface Ni was leached into the liquid phase, and the Ni extraction rate increased at higher temperature and pressure.

In the second stage, the surface Cu was extracted into the H_2SO_4+H_2O_2 solvent, while the coated Au was further delaminated in the form of solid residues as shown in Figures 3 and 10. It is important to note that the concentrations of H_2SO_4 and H_2O_2 used in our technology were as much as three times lower than those used in the literature with similar extraction rates (discussed in Figure 8. As shown in Figure 12, after the two-step WPCB treatment process, there will be four major products including solid particulates of Au and the first liquid product rich in Ni from the 1st stage treatment as well as the second liquid product rich in Cu from the 2nd stage treatment.

Given the physical and chemical alterations of the polymer-metal matrix of the WPCB found in this study, we propose to perform the $scCO_2$/acid pre-treatment prior to the grinding and homogenization processes. After the $scCO_2$-acid treatments described in this study, the residue WPCB would have a higher porosity and reduced flexural modulus (Figure 7), which may reduce the energy intensity of the subsequent grinding and homogenization processes.[89] The Cu leaching from ground WPCB would also be strongly influenced by the size and porosity of the WPCB particles. As shown in Figure 9, after Au is hydrometallurgically delaminated, Cu can be rapidly extracted from ground WPCB that was treated using $scCO_2$/acid. The final solid residue shown at the end of the process in Figure 12 would mainly contain polymeric compounds including flame retardant (e.g., Br-containing polymers). Thus, the subsequent treatment of the solid residue such as pyrolysis[90,91] should be carefully designed considering ultimate environmental and health impacts of the developed technology to address any potential toxic emission during its conversion.

In terms of the economic feasibility of this technology, $scCO_2$ should be recycled after its use in the pre-treatment unit. One of the options would be phase separation using the density difference between CO_2 and acid. By tuning the system pressure, the density of CO_2 can be controlled to achieve effective phase separation from the acid. Compared to other supercritical fluids, temperature and pressure conditions required for $scCO_2$ (31 °C and 74 bar) are relatively mild (e.g., supercritical water requires 374 °C and 221 bar).[92,93] $scCO_2$ is already being used in a number of successful commercial applications including the decaffeination process of coffee and tea.[94,95] Thus, we believe that the use of $scCO_2$ in metal recovery from WPCBs could also be economically beneficial as long as CO_2 recycling system can be carefully designed. A Detailed techno-economic analysis as well as life cycle assessment is recommended for future studies.

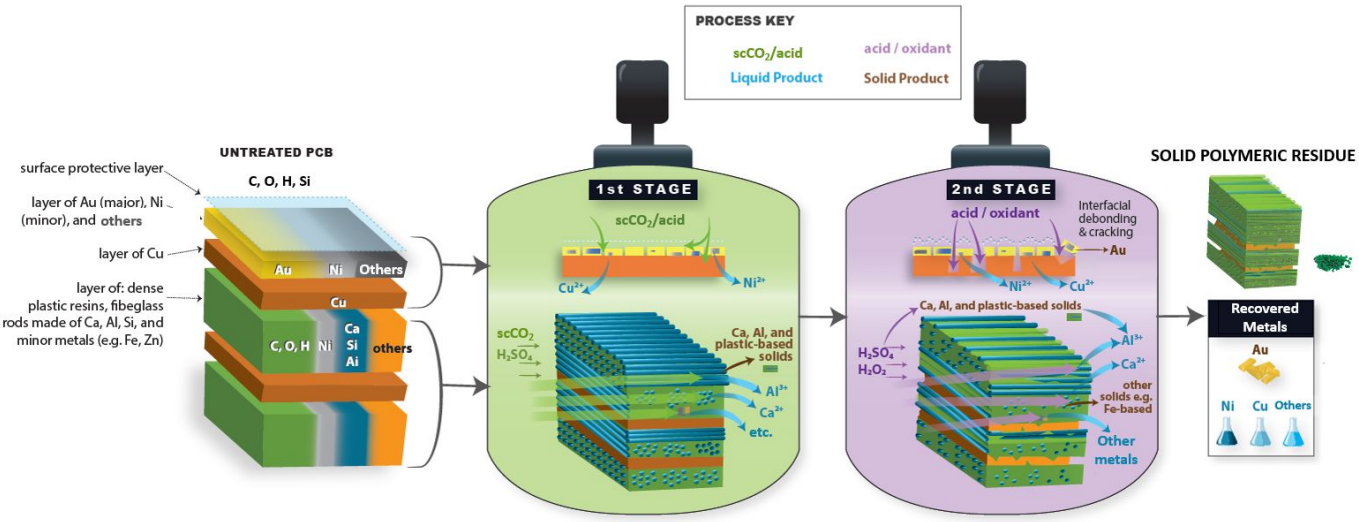

Figure 12 Summative structural and chemical alteration mechanisms of the two-stage $scCO_2$-induced printed circuit board (PCB) treatment technology

4 Conclusions

This study focused on the investigation of the synergistic physical and chemical alterations of the polymer-metal matrix in WPCBs via two-stage $scCO_2$-based solvent systems. The main chemical and physical changes in the first stage $scCO_2$+acid treatment included the foaming and fracture of the surface polymeric protective layer, as well as the formation of micron-sized pores resulting from the dissolution of Ca and Al-bearing fiberglass. The second stage acid/oxidant treatment performed under moderate concentrations (greener compared to conventional hydrometallurgical solvents) resulted in the further delamination of the outer polymer coating and beneath Au located on the surface of WPCB. The proposed two-step treatment allowed selective extractions Ni and Cu in the first

and second stages, respectively, and thus, making any subsequent separation processes easier (e.g., electrowinning of Ni and Cu). The $scCO_2$-based treatment also led to a significant decrease in mechanical strength of WPCB, which could potentially reduce the energy penalty associated with grinding of WPCBs. The proposed $scCO_2$-based treatment technology demonstrated a greener pathway to recover metals (e.g., Au, Cu and Ni) from WPCBs by replacing highly hazardous conventional cyanide and aqua regia solvents with the combination of $scCO_2$, H_2SO_4 and H_2O_2 solvents. The solvent requirement was minimized by increasing the metal recovery rate through the alteration of the structure of surface polymer layers and the dissolution of embedded Ca- and Al-bearing fiberglass in the presence of $scCO_2$. The fate of Au was also significantly different in this scheme. By recovering Au as solids rather than dissolved ions, additional separation and recovery steps for Au were eliminated making the overall WPCB treatment technology more intensified and sustainable. Lastly, the recovery of Au before the size reduction step avoided the precious metal loss due to the size reduction treatment. Future research should aim to reduce the toxicity of the developed solvent systems, to design the treatment process for the remaining polymeric residues, as well as to perform a detailed process design cost analysis that incorporates the solvent recycling and waste management.

Conflicts of interest

There are no conflicts to declare.

Acknowledgements

The authors acknowledge NSF (CBET 1706905) for financially supporting this work. The authors would like to acknowledge Adrian M Chitu for the AFM work in the Materials Science Teaching/Facility Laboratory at Columbia University.

Notes and references

1. Y. Li, M. Lin, Z. Ni, Z. Yuan, W. Liu, J. Ruan, Y. Tang and R. Qiu, *Journal of Hazardous Materials*, 2020, **386**, 121020.
2. A. Kumari, M. K. Jha, R. P. Singh and S. Ranganathan, *Heat and Mass Transfer*, 2017, **53**, 1247-1255.
3. E. Hsu, K. Barmak, A. C. West and A.-H. A. Park, *Green chemistry*, 2019, **21**, 919-936.
4. D. Lee, D. Offenhuber, F. Duarte, A. Biderman and C. Ratti, *Waste management*, 2018, **72**, 362-370.
5. C. Baldé, V. Forti, V. Gray, R. Kuehr and P. Stegmann, *Bonn/Geneva/Vienna*, 2017.
6. J. J. Licari and D. W. Swanson, in *Adhesives Technology for Electronic Applications*, eds. J. J. Licari and D. W. Swanson, William Andrew Publishing, Norwich, NY, 2005, DOI: https://doi.org/10.1016/B978-081551513-5.50009-7, pp. 393-430.
7. I. O. Ogunniyi and M. K. G. Vermaak, *Minerals Engineering*, 2009, **22**, 378-385.
8. A. Holden, J. S. Park, V. Chu, M. Kim, G. Choi, Y. Shi, T. Chin, C. Chun, J. Linthicum and B. J. Walton, *Environmental Toxicology and Chemistry: An International Journal*, 2009, **28**, 1906-1911.
9. D. Chen and R. C. Hale, *Environment international*, 2010, **36**, 800-811.
10. S. D. Shaw and K. Kannan, *Reviews on Environmental Health*, 2009, **24**, 157-230.
11. J. DiGangi, A. Blum, Å. Bergman, C. A. de Wit, D. Lucas, D. Mortimer, A. Schecter, M. Scheringer, S. D. Shaw and T. F. Webster, *Journal*, 2010.
12. P. Kiddee and S. Decharat, *Environmental earth sciences*, 2018, **77**, 456.
13. J. Hao, Y. Wang, Y. Wu and F. Guo, *Resources, Conservation and Recycling*, 2020, **157**, 104787.
14. M. Kaya, in *Electronic Waste and Printed Circuit Board Recycling Technologies*, Springer, 2019, pp. 33-57.
15. T. Hino, R. Agawa, Y. Moriya, M. Nishida, Y. Tsugita and T. Araki, *Journal of material cycles and waste management*, 2009, **11**, 42-54.
16. C. Vasile, M. Brebu, M. Totolin, J. Yanik, T. Karayildirim and H. Darie, *Energy & fuels*, 2008, **22**, 1658-1665.
17. G. Zhou, Z. Luo and X. Zhai, 2007.
18. C. Hageluken, 2007.
19. R. Khanna, G. Ellamparuthy, R. Cayumil, S. Mishra and P. Mukherjee, *Waste Management*, 2018, **78**, 602-610.
20. X. Zeng, J. A. Mathews and J. Li, *Environmental science & technology*, 2018, **52**, 4835-4841.
21. I. D'Adamo, F. Ferella, M. Gastaldi, F. Maggiore, P. Rosa and S. Terzi, *Resources, Conservation and Recycling*, 2019, **149**, 455-467.
22. R. K. Nekouei, I. Tudela, F. Pahlevani and V. Sahajwalla, *Current Opinion in Green and Sustainable Chemistry*, 2020.
23. C. Zhou, Y. Pan, M. Lu and C. Yang, *Journal of hazardous materials*, 2016, **311**, 203-209.
24. S. Chatterjee and K. Kumar, *International Journal of Physical Sciences*, 2009, **4**, 893-905.
25. J. Li, P. Shrivastava, Z. Gao and H.-C. Zhang, *IEEE transactions on electronics packaging manufacturing*, 2004, **27**, 33-42.
26. J. Guo, J. Guo and Z. Xu, *Journal of Hazardous materials*, 2009, **168**, 567-590.
27. J. Szałatkiewicz, *Materials*, 2016, **9**, 683.
28. H. S. Park, Y. S. Han and J. H. Park, *ACS Sustainable Chemistry & Engineering*, 2019, **7**, 14119-14125.
29. H. Li, J. Eksteen and E. Oraby, *Resources, Conservation and Recycling*, 2018, **139**, 122-139.
30. J. Bai, G. Weihua, L. Changzhong, Y. Wenyi, Z. Chenglong, W. Jingwei, D. Bin and S. Kaimin, in *Industrial and Municipal Sludge*, Elsevier, 2019, pp. 525-551.
31. S. Yousefzadeh, K. Yaghmaeian, A. H. Mahvi, S. Nasseri, N. Alavi and R. Nabizadeh, *Journal of Cleaner Production*, 2019, 119401.
32. H. Li, E. Oraby and J. Eksteen, *Resources, Conservation and Recycling*, 2020, **154**, 104624.
33. A. E. Ajiboye, F. E. Olasehinde, O. A. Adebayo, O. J. Ajayi, M. K. Ghosh and S. Basu, *Recycling*, 2019, **4**, 36.
34. C. Fleming, *Hydrometallurgy*, 1992, **30**, 127-162.
35. R. Montero, A. Guevara and E. dela Torre, *Journal of Earth Science and Engineering*, 2012, **2**, 590.
36. P. M. H. Petter, H. M. Veit and A. M. Bernardes, *Rem: Revista Escola de Minas*, 2015, **68**, 61-68.

37. H. Elomaa, S. Seisko, T. Junnila, T. Sirviö, B. Wilson, J. Aromaa and M. Lundström, *Recycling*, 2017, **2**, 14.
38. U. Jadhav and H. Hocheng, *Scientific reports*, 2015, **5**, 14574.
39. A. C. Kasper, J. Carrillo Abad, M. Garcia Gabaldon, H. M. Veit and V. Perez Herranz, *Waste Management & Research*, 2016, **34**, 47-57.
40. A. Tripathi, M. Kumar, D. Sau, A. Agrawal, S. Chakravarty and T. Mankhand, *International Journal of Metallurgical Engineering*, 2012, **1**, 17-21.
41. V. H. Ha, J.-c. Lee, T. H. Huynh, J. Jeong and B. Pandey, *Hydrometallurgy*, 2014, **149**, 118-126.
42. S. Camelino, J. Rao, R. L. Padilla and R. Lucci, *Procedia Materials Science*, 2015, **9**, 105-112.
43. S. Jeon, C. B. Tabelin, H. Takahashi, I. Park, M. Ito and N. Hiroyoshi, *Waste management*, 2018, **81**, 148-156.
44. W. Zhang, J. Ren, S. Liu and Z. Yuan, *Procedia Environmental Sciences*, 2016, **31**, 171-177.
45. T. Gamse, F. Steinkellner, R. Marr, P. Alessi and I. Kikic, *Industrial & engineering chemistry research*, 2000, **39**, 4888-4890.
46. C. O. Calgaro, D. F. Schlemmer, M. M. Bassaco, G. L. Dotto, E. H. Tanabe and D. A. Bertuol, *Journal of CO2 Utilization*, 2017, **22**, 307-316.
47. H.-C. Zhang, X. Ouyang and A. Abadi, 2006.
48. C. Calgaro, D. Schlemmer, M. Da Silva, E. Maziero, E. H. Tanabe and D. A. Bertuol, *Waste management*, 2015, **45**, 289-297.
49. M. Kaya, *Waste management*, 2016, **57**, 64-90.
50. J. F. Moulder, W. F. Stickle, P. E. Sobol and K. D. Bomben, *Perkin-Elmer Corp., Eden Prairie, MN*, 1992.
51. A. Wright, *Epec Engineered Tecnologies*, 2015, 1-15.
52. S. V. Levchik and E. D. Weil, *Polymer International*, 2004, **53**, 1901-1929.
53. P. Murias, H. Maciejewski and H. Galina, *European Polymer Journal*, 2012, **48**, 769-773.
54. E. D. Weil and S. Levchik, *Journal of fire sciences*, 2004, **22**, 25-40.
55. H.-C. Zhang, C.-N. Yu, Y. Liang, G.-X. Lin and C. Meng, *Polymers*, 2019, **11**, 89.
56. G. Wang, L. Xiao, Z. Liu, Z. Han, J.-H. Ouyang and D. Zhang, *Corrosion Science*, 2016, **113**, 180-182.
57. M. Antler, *IEEE Transactions on Parts, Hybrids, and Packaging*, 1974, **10**, 11-17.
58. L. Gautier, B. Mortaigne and V. Bellenger, *Composites Science and Technology*, 1999, **59**, 2329-2337.
59. Y. Li, Y. Yu, X. Jia, S. Duan and X. Yang, *Polymer Composites*, 2011, **32**, 1953-1960.
60. J. Shen, X. He and E. Li, 2018.
61. D. Chang, F. Bai, Y. Wang and C. Hsiao, 2004.
62. T. Oka, K. Ito, C. He, C. Dutriez, H. Yokoyama and Y. Kobayashi, *The Journal of Physical Chemistry B*, 2008, **112**, 12191-12194.
63. B. Ghosh, M. Ghosh, P. Parhi, P. Mukherjee and B. Mishra, *Journal of Cleaner Production*, 2015, **94**, 5-19.
64. M. El-Hadek and H. Tippur, *Journal of materials science*, 2002, **37**, 1649-1660.
65. C. Creighton and T. Clyne, *Composites Science and Technology*, 2000, **60**, 525-533.
66. A. Ucyildiz and I. Girgin, *Physicochemical Problems of Mineral Processing*, 2017, **53**, 475-488.
67. H. Yang, J. Liu and J. Yang, *Journal of hazardous materials*, 2011, **187**, 393-400.
68. E.-y. Kim, M.-s. Kim, J.-c. Lee and B. Pandey, *Journal of hazardous materials*, 2011, **198**, 206-215.
69. M. G. Hasab, F. Rashchi and S. Raygan, *Hydrometallurgy*, 2014, **142**, 56-59.
70. B. Xu, W. Kong, Q. Li, Y. Yang, T. Jiang and X. Liu, *Metals*, 2017, **7**, 222.
71. J. R. Peeters, P. Vanegas, J. R. Duflou, T. Mizuno, S. Fukushige and Y. Umeda, *CIRP Annals*, 2013, **62**, 35-38.
72. A. Marra, A. Cesaro and V. Belgiorno, *Journal of Cleaner Production*, 2018, **186**, 490-498.
73. J. Bachér, A. Mrotzek and M. Wahlström, *Waste management*, 2015, **45**, 235-245.
74. O. O. Oluokun and I. O. Otunniyi, *Hydrometallurgy*, 2020, 105320.
75. M. Sethurajan and E. D. van Hullebusch, *Metals*, 2019, **9**, 1034.
76. W. Song, M. Yoshitake, S. Bera and Y. Yamauchi, *Japanese journal of applied physics*, 2003, **42**, 4716.
77. E. Voogt, A. Mens, O. Gijzeman and J. Geus, *Surface science*, 1996, **350**, 21-31.
78. C. Yuan and Q. Zhai, *Recycling Printed Circuit Board Wastes Through Supercritical Fluid Delaminating*, University of Wisconsin-Milwaukee, University of Wisconsin System Solid Waste Research Program, 2011.
79. S. Sanyal, Q. Ke, Y. Zhang, T. Ngo, J. Carrell, H. Zhang and L. L. Dai, *Journal of cleaner production*, 2013, **41**, 174-178.
80. D. Lefebvre, B. Ahn, D. Dillard and J. Dillard, *International journal of fracture*, 2002, **114**, 191-202.
81. J. Bouchet, A. Roche and E. Jacquelin, *Journal of adhesion science and technology*, 2001, **15**, 321-343.
82. M. Yuedong, F. Futang and P. Chang, *Journal*, 2018.
83. G. R. Allardyce, A. J. Davies, D. J. Wayness and A. Singh, *Journal*, 1992.
84. F. T. Wallenberger and P. A. Bingham, *Energy-Friendly Compositions And Applications*, 2010.
85. R. Jones and J. Stewart, *Journal of non-crystalline solids*, 2010, **356**, 2433-2436.
86. J. D. Tanks, Y. Arao and M. Kubouchi, *Composite Structures*, 2018, **202**, 686-694.
87. H. Li, P. Gu, J. Watson and J. Meng, *Journal of Materials Science*, 2013, **48**, 3075-3087.
88. Y. Zhao, Z. Shen, Z. Tian, W. Huang, J. Wu and Z. Fan, *Journal of Non-Crystalline Solids*, 2019, **511**, 212-218.
89. H. Tomino, A. Tsukuda, Y. Kondo and K. Ishizaki, *Journal of the Japan Society of Powder and powder Metallurgy*, 1999, **46**, 257-261.
90. Y. Shen, X. Chen, X. Ge and M. Chen, *Journal of environmental management*, 2018, **214**, 94-103.
91. C. Ma, J. Yu, B. Wang, Z. Song, J. Xiang, S. Hu, S. Su and L. Sun, *Renewable and Sustainable Energy Reviews*, 2016, **61**, 433-450.
92. G. Sapkale, S. Patil, U. Surwase and P. Bhatbhage, *Int. J. Chem. Sci*, 2010, **8**, 729-743.
93. K. Ehara and S. Saka, ACS Publications, 2004.
94. N. Rozzi and R. Singh, *Comprehensive reviews in food science and food safety*, 2002, **1**, 33-44.
95. D. Villanueva, P. Luna, M. Manic, V. Najdanovic–Visak and T. Fornari, *food processing*, 2011, **1**, 3.